Science of the Total Environment 670 (2019) 466–477

Contents lists available at ScienceDirect

Science of the Total Environment

journal homepage: www.elsevier.com/locate/scitotenv

Altitudinal disparity in growth of Dahurian larch (*Larix gmelinii* Rupr.) in response to recent climate change in northeast China

Xueping Bai [a,b], Xianliang Zhang [b,d], Junxia Li [a,b], Xiaoyu Duan [b], Yuting Jin [b], Zhenju Chen [a,b,c,*]

[a] College of Land and Environment, Shenyang Agricultural University, Shenyang 110866, China
[b] Tree-Ring Laboratory/Research Station of Liaohe-River Plain Forest Ecosystem CFERN, College of Forestry, Shenyang Agricultural University, Shenyang 110866, China
[c] Qingyuan Forest CERN, Chinese Academy of Sciences, Shenyang 110164, China
[d] College of Forestry, Hebei Agricultural University, Baoding 071001, China

HIGHLIGHTS

- The larch growth decline at low altitude and increase at high altitude.
- Effects of summer temperature/precipitation on growth at high altitude was opposite to that at low altitude.
- The response shift threshold of larch to temperature and precipitation of ca. −4 °C and ca. −5 °C, respectively.
- The larch radial growth changed from the temperature limit at high altitude to the drought limit at low altitude.

GRAPHICAL ABSTRACT

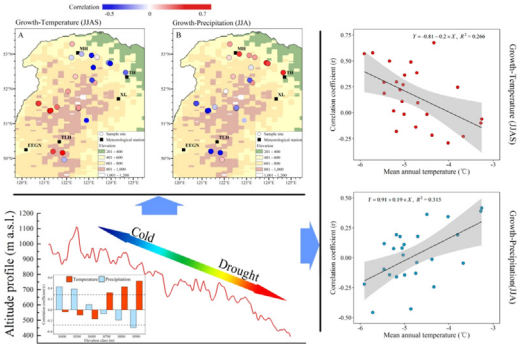

ARTICLE INFO

Article history:
Received 1 December 2018
Received in revised form 14 March 2019
Accepted 15 March 2019
Available online 16 March 2019

Editor: Elena Paoletti

Keywords:
Dahurian larch
Radial growth
Climate change
Temperature thresholds
Altitude gradient

ABSTRACT

Forests are sensitive to climate change at high altitude and high latitude. Dahurian larch (*Larix gmelinii* Rupr.) has experienced an unprecedented forest retreat northward during the last century. Whether the response of growth to climate has dissimilar patterns at different altitudes, and what the "altitudinal trends" of forest development will be in the future, remains unclear. We dendroclimatically investigated the impacts of climate change on the growth of larch forests along an altitudinal gradient. In total, 721 trees from 25 forest stands, representing an altitudinal range from 400 to 950 m a.s.l. in the Great Xing'an Mountains, northeast China, were sampled and used to develop tree-ring width chronologies. The results suggest that warming caused a decline in larch growth at low altitude, while tree growth increased at high altitude. The growth–climate relationships indicate that October–February temperatures were positively correlated with larch growth at low- and high-altitude sites, but negatively correlated at medium-altitude sites (ca. 600–700 m a.s.l.). April–May (early spring) temperatures and October–January precipitation had positive effects on growth in general (ca. 75% of all sites). The effects of summer temperature/precipitation on larch growth at high-altitude sites were opposite to that at low-altitude sites. This change of response from significantly positive/negative correlation to significantly negative/positive correlation occurred gradually along the altitudinal gradient. The relationships varied significantly with altitude both in the case of temperature ($R^2 = 0.425$, $P < 0.001$) and precipitation ($R^2 = 0.613$, $P < 0.001$). The shift in response of larch forest to changes in summer temperature and precipitation occurred in the areas

* Corresponding author at: College of Forestry, Shenyang Agricultural University, Shenyang 110866, China.
E-mail address: chenzhenjuf@163.com (Z. Chen).

https://doi.org/10.1016/j.scitotenv.2019.03.232

with a mean annual temperature of ca. −4 °C and ca. −5 °C, respectively; larch growth at temperatures lower or higher than these thresholds was limited by temperature and precipitation, respectively.

1. Introduction

Climate change is altering the growth and geographical distribution of plants (I. Chen et al., 2011; Moritz and Agudo, 2013; Kueppers et al., 2017), and causing changes in the long-term persistence of many species. For example, the warming climate has not only caused trees to shift their distributions to high altitudes and high latitudes (I. Chen et al., 2011; IPCC, 2013; Morgan et al., 2014; Schwörer et al., 2014), but has also exacerbated water limitations, for instance by causing permafrost degradation that can be a fatal blow to the forest (Wei et al., 2011; Baltzer et al., 2014). Indeed, there is much documented evidence at both a regional and global scale that woody plants are affected by global warming (Beckage et al., 2008; Moritz and Agudo, 2013; Vicente-Serrano et al., 2013; Williams et al., 2013; Martin-Benito and Pederson, 2015; Wason and Dovciak, 2016). This includes, in particular, the divergence of tree growth caused by differences in local microtopographies or micro-climate during recent decades (Driscoll et al., 2005; Martin-Benito and Pederson, 2015; Bai et al., 2016), and the specific response patterns of growth–climate relationships and their driving mechanisms worldwide (e.g., Linares and Tíscar, 2011; Jyske et al., 2014; Jiang et al., 2016; Suvanto et al., 2016; Wang et al., 2016). Previous studies have also shown that tree growth has a strong dependence on summer water availability and that water stress is increasing tree mortality at lower altitudes (van Mantgem et al., 2009; Vicente-Serrano et al., 2013; Kolář et al., 2017). High-altitude tree growth has been found to have a positive growth trend with a higher positive correlation with growing season temperature compared to low-altitude sites, growth at the latter having a stronger negative correlation with temperature (Lyu et al., 2017; Matías et al., 2017). The use of massive samples when studying regional and hemispherical forest dynamics and ecological processes has helped us to precisely quantify many biogeographical patterns, such as the geographical variation in growth–climate relationships (Vicente-Serrano et al., 2013; Suvanto et al., 2016; Matías et al., 2017). Massive collections of samples and their subsequent analysis also help us to better estimate or understand the specifically ecological potential of forest dynamics and the geographical distribution of vegetation under different climate scenarios in the future.

For any particular tree species, the limiting factors shift across the altitudinal gradient from water stress at low altitude to low-temperature limitation at high altitude (Salzer et al., 2009; Babst et al., 2013; Vicente-Serrano et al., 2013), especially in the temperate and boreal forest. The general movement of species distributional ranges in a particular period, as a biogeographical model, can help us to understand the response of growth to climate change, but is too simplistic for the assessment of forest persistence and loss (Jump et al., 2009; Rabasa et al., 2013). Changes in the ecological environment are a combined effect of multi-dimensional and complex natural elements at high altitudes and latitudes, rather than simply direct effects of regional climate alone. For example, the degeneration of permafrost and advancement of snow melt (time) due to climate change (Kirdyanov et al., 2003; Clow, 2010) cause transitions in hydrothermal conditions and soil physicochemical properties, and then affect the water-use efficiency, photosynthesis, respiration and carbon accumulation of trees (Goodine et al., 2008; Sulman et al., 2016; Zhang et al., 2018b). Therefore, non-climate environmental factors should be taken into account when identifying the main climate drivers of forests or assessing the likely impacts of future climate on tree growth. On the other hand, species distributions are mainly affected by regional climate dynamics, which can be explored through the past climate response and tree ontogeny trends of forests (Rabasa et al., 2013; Schwörer et al., 2014) and can be identified via the climatic driving threshold of species distribution range along an altitudinal gradient (Matías et al., 2017). It is this kind of climate driving threshold that can be regarded as the forewarning level of forest persistence in a warming future climate.

Dahurian larch (*Larix gmelinii* Rupr.) is one of the most important species growing in the forest ecosystems in northeast Asia, with the most southerly extent of its range being the Small and Great Xing'an Mountains, China. The entire distribution of larch in China is at the southeastern margin of the Eurasian cryolithozone (Wei et al., 2011). Dahurian larch extends to the southern high-altitude area of northeast China (Leng et al., 2008a) due to the decrease in temperature with increasing altitude (Jump et al., 2009). Permafrost, the maintenance system of the Dahurian larch ecosystem, is being degraded and the southern boundary is moving northward in the context of global warming (Wei et al., 2011). At the same time, the response of Dahurian larch growth to climate has become more complicated in recent decades, with summer temperature, for example, having positive and negative correlations with larch radial growth in permafrost (Zhang et al., 2011; Chen et al., 2013; Zhang et al., 2018a) and non-permafrost stands (Bai et al., 2016), respectively. Given this scenario, it is essential to consider the importance of altitudinal effects—as a crucial geographical feature—on both growth-climate response patterns and the future species distribution, which has never been studied in this region. Consequently, it is also possible to use changes along altitudinal gradients as a proxy for temporal changes with climate over a specific period. For example, changes in growth-climate response of Dahurian larch communities across an altitudinal gradient can be used to evaluate the local hydrothermal conditions and accompanying changes in permafrost environments and forest distributions under global warming.

Tree rings can be used as a tool to indicate long-term, historical forest ecosystem dynamics, to assess the impacts of climate warming on tree growth further, and to forecast the potential variations in forests with future climate change (Fritts, 1976; Salzer et al., 2009). In this study, we set up a tree-ring width network and conducted dendroclimatic investigations on Dahurian larch in a boreal forest area with an altitudinal gradient ranging from 400 m to 950 m a.s.l. in northeast China. Our hypothesis is that Dahurian larch has dissimilar radial growth patterns and different growth-climate relationships along the altitudinal gradients. The results will have profound implications for the understanding of forest development trends and the terrestrial carbon cycle, as well as for species distributional ranges and forest management practices under a warming climate. Our objectives were (1) to explore the varied patterns of tree growth along altitudinal gradients affected by climate gradients; (2) to investigate changes in the growth-climate relationship with altitude; and (3) to assess response (shift) thresholds driven by changing climate.

2. Materials and methods

2.1. Study area

Our study area (49°57′N–53°13′N, 120°44′E–124°41′E) is located on the Great Xing'an Mountains in northeast China (Fig. 1A). Dahurian larch is the dominant tree species in this area, forming light coniferous forests as a part of the world's boreal forest, which is highly sensitive to temperature variations (Zhang et al., 2016). The average duration of the Dahurian larch growth season is ca.165 days (from early May to mid-October). Forest stands are subjected to discontinuous and continuous permafrost, and are located within altitudes of 300–1200 m above sea level (a.s.l.). Our sample sites are located on both continuous and

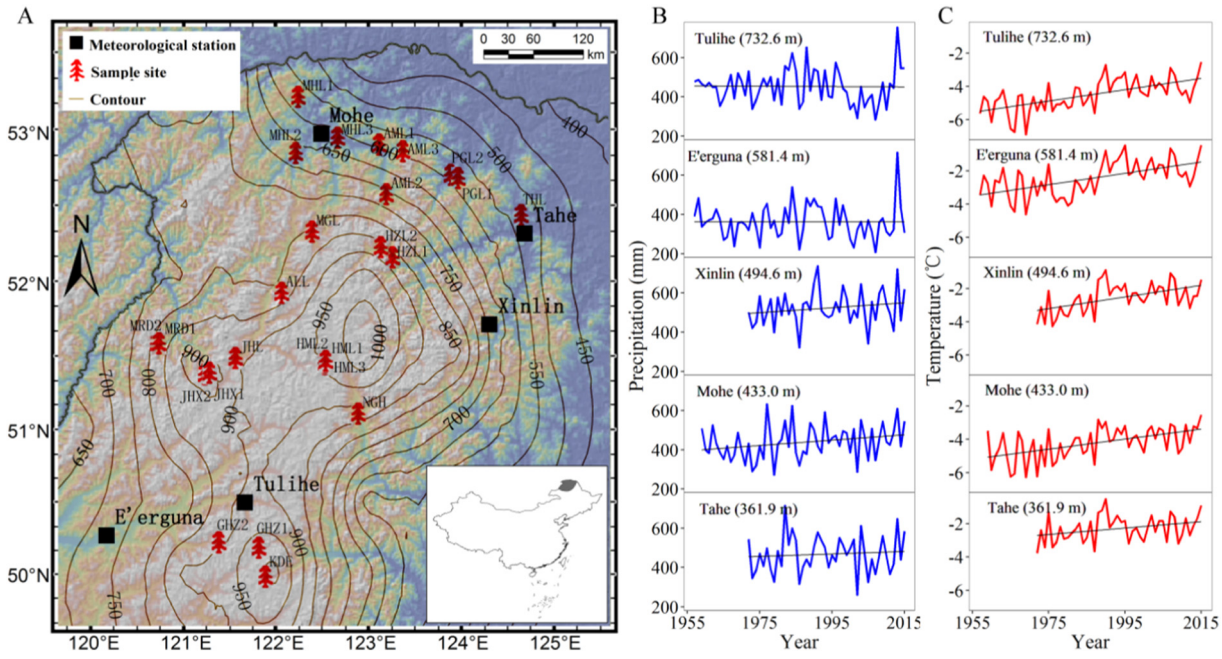

Fig. 1. Distribution of sample sites and meteorological stations (A). Solid curves represent the altitude contours at 50 m intervals. The inset map shows the location of the study area (shaded in grey) within China. Temporal changes of annual total precipitation (B) and mean annual temperature (C) at five meteorological stations in the study area. Black lines represent the linear trend. The altitude of each meteorological station is given in parentheses.

discontinuous permafrost regions in the south and northeast of Great Xing'an Mountains, respectively (Guo et al., 2015). The study area is largely subject to a cold-temperate continental monsoon climate. According to the climate records (1957–2015) of five local meteorological stations, the mean annual temperature is −3.2 °C with January and July being the coldest (mean −27.5 °C) and warmest (mean 18.2 °C) months, respectively. Mean annual temperature is −4.5 °C at Tulihe, the highest meteorological station, and −2.2 °C at Tahe, the lowest meteorological station. All the single station mean annual temperature records show an obvious long-term positive trend (Fig. 1C). The altitude decreases from south to north (from 950 to 400 m a.s.l.) within a small latitude span, from 50° N to 53° N across the study area. A "cold island" is formed in the south where the temperatures are particularly lower than those in the northern part of the study area (Fig. 1A). Because temperature decreases by 1 °C with an increase of ca. 167 m in altitude (Jump et al., 2009), the study area has a difference of ca. 3 °C in temperature between the highest and lowest altitude sites. Mean annual precipitation is 449 mm in the study area, with 295 mm of that coming in June to August. The maximum mean annual snow depth is 21–25 cm in February (Wei et al., 2011).

2.2. Tree-ring sampling and chronology development

Twenty-five sample sites were selected along an altitudinal range from 400 to 950 m a.s.l. to represent a wide transect of the area of Dahurian larch occurrence. Over the period 2008 to 2015, a minimum of 20 mature and healthy trees per site were cored using a 5.15 mm inner diameter increment borer at breast height (1.3 m above ground level). The sampling was undertaken in October each year and was focused in the river valley and on gentle slopes, with one to three cores taken from each tree. Each tree-ring sample collected was stored in a custom-made plastic tube and brought back to the laboratory. The samples were then subjected to a process of drying, mounting and polishing with coarse to fine sandpapers to enable the rings to be seen clearly. All cores were cross-dated under a microscope and measured using a LINTAB 5 tree-ring width measuring system (Rinntech Heidelberg, Germany) with an accuracy of 0.01 mm. The quality of the measurement series was checked using the COFECHA program (Holmes, 1983). In total, 1340 cores from 721 trees were available for the development of tree-ring width chronologies.

A signal-free method based on the program RCSsigFree v45 (http://www.ldeo.columbia.edu/tree-ring-laboratory/resources/software) was used to develop the chronologies for all sites, this dividing the common signal into original measurement data to mitigate the "end effect" of the "trend distortion" problem (Melvin and Briffa, 2008). The chronology indices were calculated by ratios of each tree-ring series. The Friedman curve-fitting method was chosen for raw tree-ring series detrending with an alpha value of 7 (Friedman tweeter); this can stabilize sharp fluctuations in the front end of the tree ring chronology due to small sample size. The mean chronology was calculated by the robust Tukey bi-weight mean. The running Rbar window width was set to 51 years for variance stabilization of calculated correlations. The age-dependent spline stabilization was selected as the additional detrending curve option. The iterated operation then proceeded with a convergence test level of 0.0001 based on minimizing the mean absolute differences between the current and proceeding chronologies. Eventually, the process resulted in the production of 25 signal-free (ssf) tree-ring width chronologies.

We also calculated basal area increments (BAI) for each tree (averaged all cores from one tree) using raw measurement width according to the following formula, and averaged the BAI for all trees in a site to form a composite site chronology, resulting in 25 BAI chronologies.

$$\mathrm{BAI} = \pi \times \left(R_n^2 - R_{n-1}^2\right)$$

where R is the radius of the tree, and n is the year of tree-ring formation.

2.3. Climate data

Climate data were obtained from the China Meteorological Data Service Center (http://data.cma.cn). The monthly mean temperature and the monthly total precipitation from five nearby meteorological stations were used for this study (Fig. 1A): E'erguna (581.4 m a.s.l.), Tulihe (732.6 m a.s.l.), Xinlin (494.6 m a.s.l.), Tahe (361.9 m a.s.l.) and Mohe station (433.0 m a.s.l.). Based on the consistency of the climate data

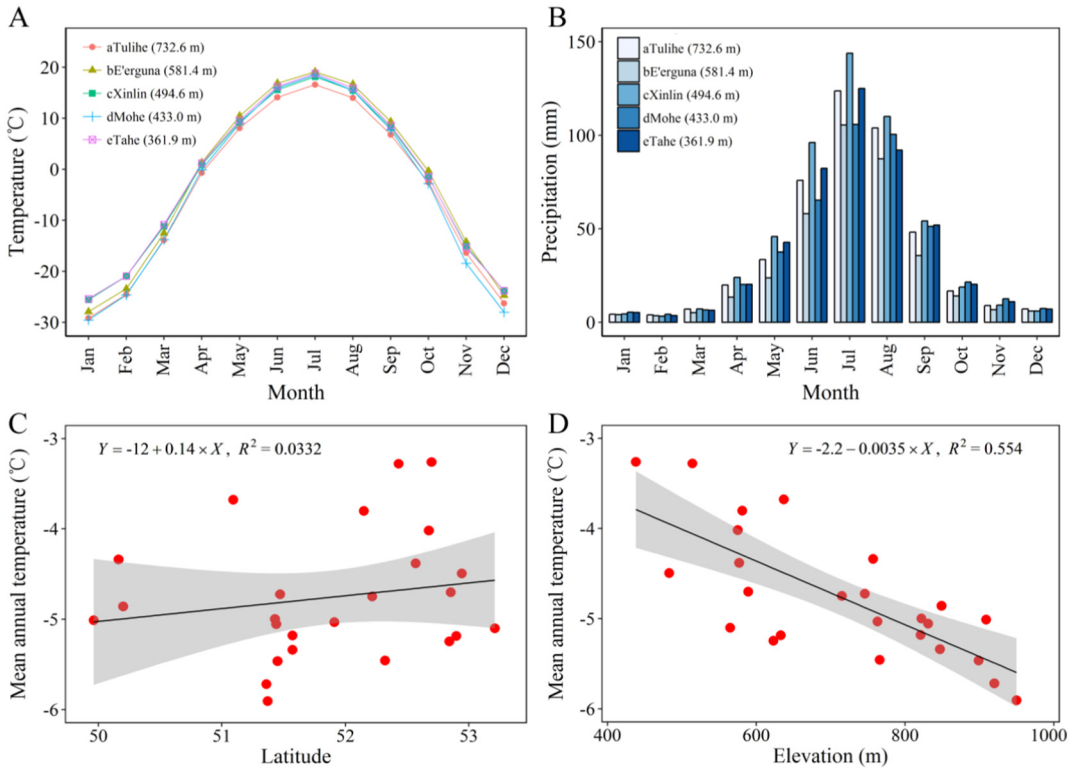

Fig. 2. Monthly mean temperature (A) and monthly total precipitation (B) at five meteorological stations; mean annual temperature (interpolated data) with increasing latitude (C) and altitude (D).

between these stations (Fig. 2A, B), averaged meteorological data were calculated for three low-altitude stations (Xinlin, Tahe and Mohe) and two high-altitude stations (E'erguna and Tulihe) from 1960 to 2008. The average data were used in subsequent dendroclimatic analysis.

According to the vertical and latitudinal lapse rate of temperature (0.6 °C/100 m or 1°) and the differences in altitude between the meteorological stations and sample sites, the mean annual temperature of each meteorological station was used to derive the mean annual temperature of each sampling site. The mean annual site temperatures were interpolated using the Inverse Distance Weighting (IDW) method (Tomczak, 1998), with the weighting power of distance designated as 2. Spatial variation in temperature along a latitudinal gradient could obviously be compensated by the effect of altitude across the study region. Although the temperatures for each sample site were obtained using a spatial-interpolation method, the interpolated data still have stepwise differences and can reflect the spatial variation including trends of actual temperature variations along the altitudinal gradient. The temperature decreased significantly with increasing altitude from north to south ($R^2 = 0.554$, $P < 0.001$; Fig. 2D), with a slightly latitudinal trend ($P = 0.38$; Fig. 2C).

2.4. Data analysis

Principal component analysis (PCA) was performed to investigate the main variance among chronologies along the altitudinal gradient. Pearson correlations between tree-ring width chronologies and monthly climate records (e.g., temperature and precipitation) from the previous September to the current October were calculated for the period 1960–2008. Moving correlations were calculated between the averaged chronologies and seasonal climate data. All analyses and charting were performed using the packages 'stats', 'ggbiplot' and 'ggplot2' in R (R Core Team, 2017). We also analyzed the spatial profile of correlation coefficients between tree-ring width index and seasonal climate variables during this period. Considering that the effect of September precipitation on growth is different from that of June to August, the combined precipitation for summer was selected as June to August (JJA), and the temperature for the growing season as June to September (JJAS). The BAI was calculated in R using the dplR package (Bunn, 2008).

3. Results

3.1. Chronology and statistics

The length of time span of Dahurian larch chronologies varied from 155 to 483 years, with the longest chronology dated back to 1532 CE. Because the main purpose of this study was to investigate the impact of altitudinal variation on radial growth and on the response of tree growth to climate, we used the latest 50 years of chronologies, covering the period 1960–2008, to match the length of the climate records (Fig. 3). Based on the correlation matrix of 25 chronologies (Fig. S1), they were merged into six composite chronology classes according to each sample site's altitude from 400 to 950 m a.s.l. (100 m per class, Table 1). Of all 25 chronologies, ca. 62% of high-altitude sites had positive growth trends whereas ca. 67% of low-altitude sites had negative growth slopes during the period 1980–2008. The BAI chronologies also had different growth trends along the altitudinal gradient in the period 1900–2008 (Fig. S2). The high-frequency variations in chronology are similar among all sites in the study area. The tree growth at the low-altitude sites showed a greater mean sensitivity (MS) and higher inter-annual fluctuations in ring-width index than that at relatively high altitudes (Table 1, Fig. 3). The expressed population signal (EPS) was the primary tool used to evaluate the common variability present in all series and to determine the reliable period of the chronologies, and the overall EPS value was above 0.85 for our 25 chronologies, at least from 1880. The first-order autocorrelation (1st AC) can reflect the influence of the previous year's climate on the growth year. The 1st AC values for our data do not vary with the altitude gradients.

The PCA of the six composite tree-ring width chronologies during the common period of 1960–2008 showed that the PC1, PC2 and PC3 accounted for 64.8%, 17.0% and 11.2%, respectively, of the total variance

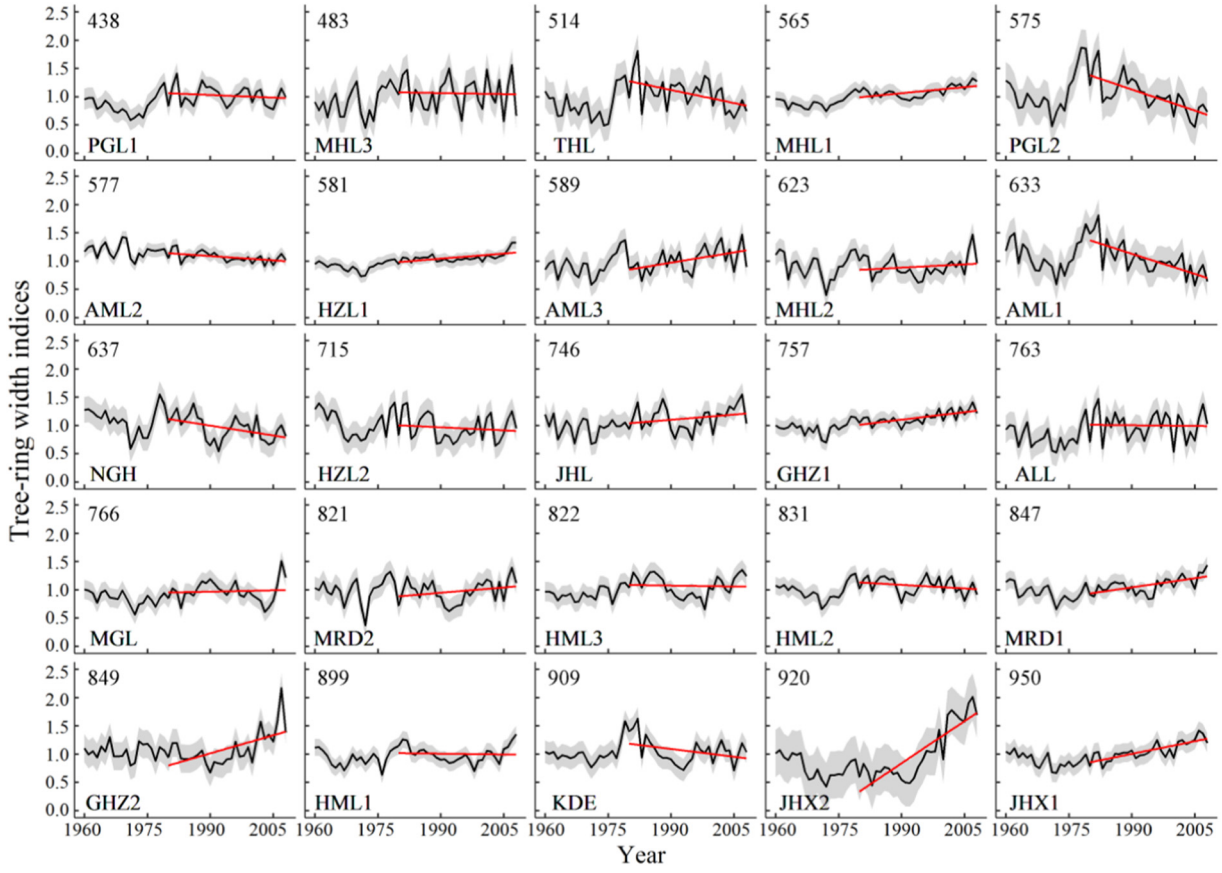

Fig. 3. Chronologies for the period 1960–2008 along an altitudinal gradient from 400 to 950 m a.s.l. The red lines indicate the growth trend during the latest 30 years. Grey areas represent the standard deviations (SD) of tree-ring width index. The altitude of the sampling site (m a.s.l.) is given at the top left each subplot. (For interpretation of the references to colour in this figure legend, the reader is referred to the web version of this article.)

in the tree-ring network (Fig. 4). They also, respectively, reflect a common growth profile of tree among all six gradients (400–900 m a.s.l.), a contrasting growth pattern among sampling sites at high and low altitudes (with a boundary of ca. 600–700 m a.s.l.), and a growth pattern at medium altitudes that is opposite to that at the high and low altitudes (ca. 400–500 m, ca. 900 m a.s.l.) in this region.

Table 1
Information on the sample sites and chronology characteristics.

Altitude classes	Site ID	Altitude (m a.s.l.)	Latitude °N	Longitude °E	Time span	Trees (cores)	MS	Standard deviation	EPS (>0.85)	1st AC
400–500	PGL1	438	52.70	123.91	1784–2015	42 (79)	0.294	0.199	0.872 (1795)	0.482
	MHL3	483	52.94	122.69	1801–2015	15 (26)	0.391	0.281	0.854 (1855)	0.236
500–600	THL	514	52.43	124.68	1675–2015	24 (59)	0.303	0.247	0.851 (1729)	0.419
	MHL1	565	53.21	122.26	1593–2014	32 (53)	0.255	0.255	0.856 (1709)	0.741
	PGL2	575	52.68	123.99	1755–2015	19 (34)	0.291	0.200	0.908 (1786)	0.432
	AML2	577	52.57	123.22	1738–2015	21 (44)	0.352	0.232	0.869 (1747)	0.407
	HZL1	581	52.15	123.28	1563–2015	42 (80)	0.266	0.293	0.867 (1750)	0.686
	AML3	589	52.85	123.39	1651–2015	25 (48)	0.340	0.193	0.852 (1791)	0.285
600–700	MHL2	623	52.84	122.23	1620–2015	26 (54)	0.266	0.217	0.851 (1692)	0.429
	AML1	633	52.90	123.14	1695–2015	23 (40)	0.327	0.206	0.886 (1764)	0.465
	NGH	637	51.09	122.91	1822–2010	53 (102)	0.266	0.186	0.878 (1872)	0.336
700–800	HZL2	715	52.22	123.16	1737–2015	26 (58)	0.253	0.178	0.853 (1762)	0.522
	JHL	746	51.47	121.58	1709–2014	30 (57)	0.303	0.221	0.866 (1740)	0.327
	GHZ1	757	50.16	121.83	1748–2008	39 (82)	0.269	0.158	0.876 (1791)	0.214
	ALL	763	51.91	122.08	1532–2014	35 (55)	0.297	0.481	0.897 (1740)	0.547
	MGL	766	52.32	122.41	1737–2014	20 (38)	0.238	0.263	0.862 (1791)	0.569
800–900	MRD2	821	51.57	120.73	1796–2008	29 (52)	0.277	0.211	0.863 (1808)	0.422
	HML3	822	51.43	122.55	1754–2013	27 (49)	0.257	0.202	0.854 (1767)	0.549
	HML2	831	51.44	122.55	1786–2013	9 (13)	0.254	0.193	0.857 (1880)	0.285
	MRD1	847	51.57	120.75	1714–2008	21 (40)	0.242	0.166	0.869 (1743)	0.435
	GHZ2	849	50.20	121.40	1592–2008	27 (38)	0.261	0.217	0.912 (1616)	0.447
	HML1	899	51.45	122.56	1827–2013	37 (63)	0.248	0.239	0.893 (1839)	0.323
900–1000	KDE	909	49.96	121.91	1859–2013	22 (46)	0.333	0.201	0.858 (1867)	0.332
	JHX2	920	51.36	121.25	1584–2013	38 (64)	0.234	0.359	0.857 (1615)	0.684
	JHX1	950	51.37	121.30	1712–2013	39 (66)	0.240	0.168	0.850 (1720)	0.334

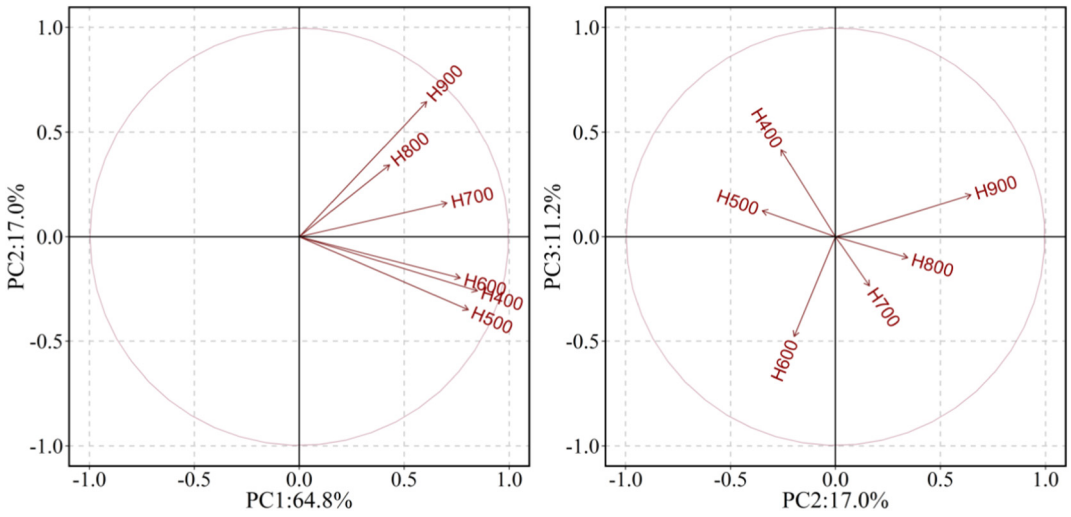

Fig. 4. The loadings of six composite chronologies on the first three principal components for the common period of 1960–2008.

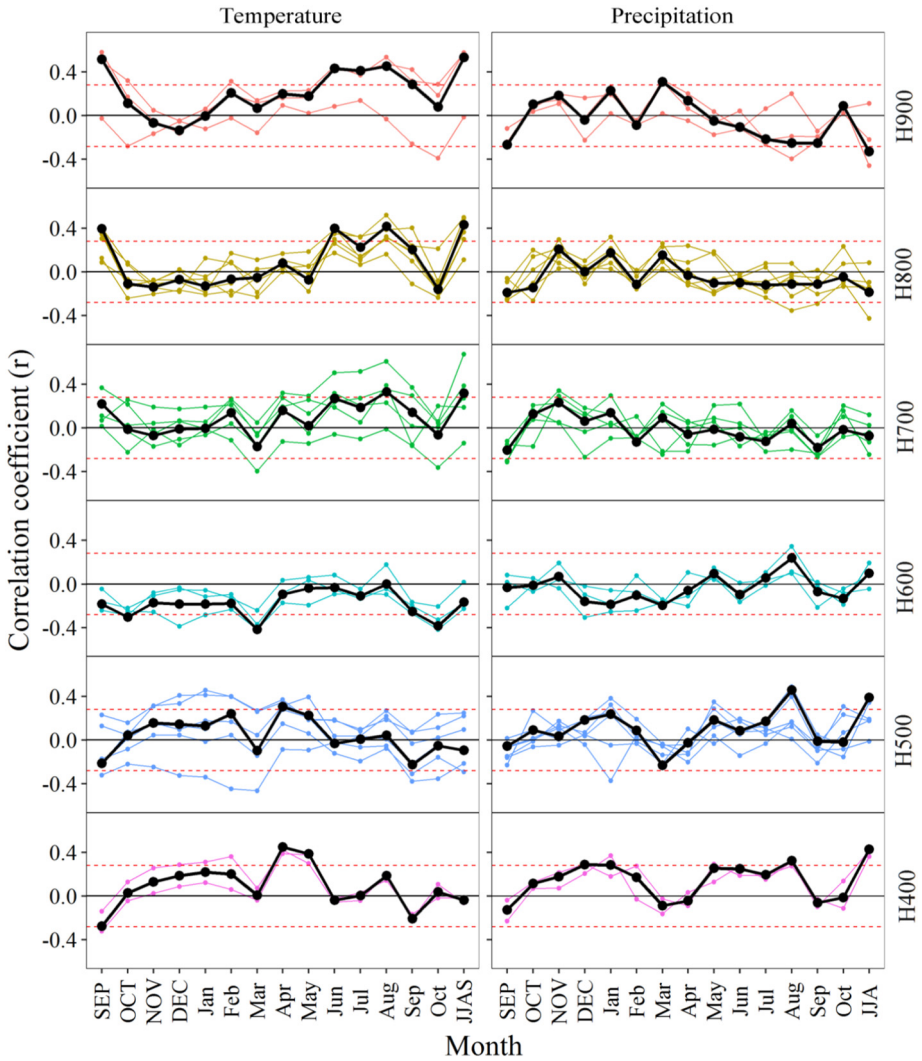

Fig. 5. Correlations between 25 chronologies and monthly climate variables from the previous September to the current October for the period 1960–2008. Colored lines represent the different altitudinal classes (400–900 m). The thick black line represents the correlation between the corresponding composite chronology and monthly climate variables in each class. Capital letters: previous year months; lowercase: current year months; JJAS denotes Jun–Sep, and JJA denotes Jun–Aug. The dashed red line represents the 95% confidence level.

3.2. Radial growth–climate relationship at different altitudes

The individual chronologies had a positive or negative correlation with climate variables along the altitudinal gradient in the growth–climate relationship analysis (Fig. 5). Temperature and precipitation had totally opposite effects at the same altitude in the growing season. October–February temperature positively affected tree growth at most high and low altitudes, while it affected tree growth negatively at medium altitudes (600–700 m a.s.l.). April–May temperature had positive effects on tree growth at 76% of all sites across the altitude range. However, June–September temperature had positive effects on tree growth at high altitude sites and negative effects at most of the low altitude sites (Fig. 5). October–January precipitation had a positive effect on tree growth at the majority of sampling sites. March precipitation showed opposite effects on tree growth along the altitudinal gradients: positive effects at high altitude sites and negative effects at low altitude sites. Precipitation in May–August showed negative effects on tree growth at high altitudes and positive effects at low altitudes (Fig. 5).

We also calculated the correlation coefficients between the composite chronologies, representing tree growth at six altitudes, and monthly climate variables (Fig. 5). The results showed a contrasting pattern of Dahurian larch growth–climate response along the altitudinal gradients. The seasonal climate and composite chronologies had a clearly diverging relationship (Fig. 6): tree growth was negatively correlated with temperature at low altitudes, and the insignificant correlation coefficients increased with increase in altitude, shifting from negative to positive ($P < 0.05$) at an altitude of ca. 600–700 m a.s.l. The profile of the growth–precipitation response is the opposite to that of growth–temperature along the altitudinal gradients. For example, summer precipitation had a positive effect on tree growth at low-altitude sites and a negative effect at high-altitude sites, and the gradual transition of correlation coefficients varied from significantly positive to insignificantly positive to insignificantly negative, and to significantly negative along the altitude gradients from 400 to 950 m a.s.l. (Fig. 6). Moving correlations between composite chronologies and seasonal climate data showed obvious changes after 1980, the correlations with temperature increasing in the period after 1980 and the correlations with precipitation decreasing (Fig. S3).

3.3. The shift of growth–climate associations along the altitudinal gradient

The spatial distribution of correlation coefficients between chronologies and climate variables was identified and displayed as a spatial profile of growth–climate relationship dynamics in the study area: summer temperature positively and negatively affected tree growth in southern high-altitude and northern low-altitude sites in the study area, respectively (Fig. 7A); summer precipitation negatively and positively affected tree growth at high-altitude and low-altitude sites, respectively (Fig. 7B). Regressions of correlations between tree growth and climate at different altitudes clearly demonstrate geographical trends in the growth-climate response in the study area; for example, the response of radial growth to temperature (JJAS) and to summer precipitation (JJA) changed significantly from negative to positive ($R^2 = 0.425$, $P < 0.001$; Fig. 7C) and from positive to negative ($R^2 = 0.613$, $P < 0.001$; Fig. 7D), respectively, with increased altitude.

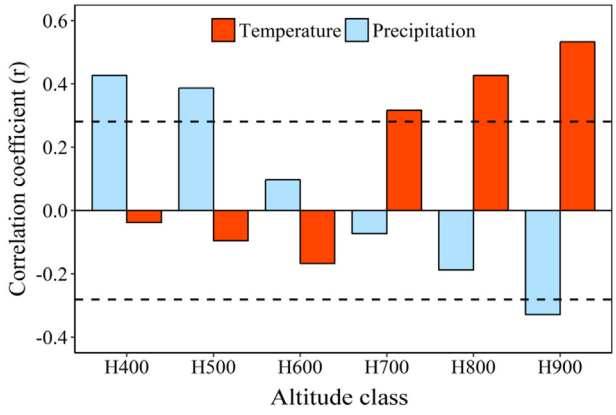

Fig. 6. Correlations between the composite chronologies and JJA precipitation/JJAS temperature for the period 1960–2008. The dashed line represents the 95% confidence level.

4. Discussion

4.1. Altitudinal divergence in growth

Large-scale studies of climate response have found that the ambient environmental condition of forests can be temperature-limited at the upper altitudinal or latitudinal limit of forest ranges, whereas the low-altitude forests are more sensitive to moisture (Harsch et al., 2009; Babst et al., 2013). But the differences in tree growth at different altitudes are widespread due to the differences in climate at different altitudes (Mátyás, 2010; L. Chen et al., 2011; Sidor et al., 2015; Matías et al., 2017). Temperature is the main climate factor that limits the growth of trees in extremely cold alpine regions (Pauli et al., 2012; Hartl-Meier et al., 2014; Suvanto et al., 2016; Matías et al., 2017). As the climate warms, forests move to higher altitudes within their geographical distribution ranges and trees that are usually located at the southern boundary of boreal forests are particularly vulnerable to the effects of warming-induced drought stress (Pauli et al., 2012; Moritz and Agudo, 2013; Kueppers et al., 2017).

In the present study, obviously divergent growth trends occurred in Dahurian larch at the southern boundary of its distributional range: larch radial growth showed positive trends at high altitude and negative trends at low altitude over the last 30 years (Fig. 3). The mean annual temperature varies by ca. 3 °C between high and low altitude, so the effects of altitude-related temperature difference on tree growth obscure those related to latitude, particularly in this area, indicating the dominance of temperature restriction on larch growth compared to other environmental factors (e.g., topography and biological factors). The growth–climate divergence is also well displayed in principal component analysis of radial-growth variations. PC2 indicate that growth patterns in trees at low altitude were the opposite to those at high altitude in the study area, although PC1 represented a common signal accounting for a greater amount of the total variance among all sites (Fig. 4). The geographical differences in growth–temperature response indicate a low-temperature constraint in high altitude forests in the southern part of the study area and a sensitivity to moisture in forests growing in the northern part.

In the context of global warming, there was a significant increase in temperature around the 1980s; for example, mean annual temperature increased from −4.3 °C to −2.9 °C in the study area (data from meteorological stations). Despite global warming currently showing signs of a "slowdown" or "hiatus" (IPCC, 2013; Kosaka and Xie, 2013)—this being a topic that is subject to emerging discussions (Karl et al., 2015)—the present study showed forests exhibiting different growth patterns in response to climate across the study area. Under warming conditions, the low-temperature limiting effect on tree growth was released at high altitude and the moisture stress increased at low altitude. This is consistent with the findings of many studies, such as the positive growth trends found to occur in the tree line and expansion of tree distribution to higher altitudes (Matías et al., 2017), the strong dependence of tree-ring growth on summer water availability (Kolář et al., 2017), and drought-limitation increases at low altitude (Vicente-Serrano et al., 2013). In addition, the warming climate leads to the dramatic degradation of permafrost over different time scales along the altitudinal gradient, resulting in two opposite hydrothermal patterns for high- and low-altitude forests. Permafrost at the current air temperature is susceptible to thawing due to a higher ground temperature, which has resulted in

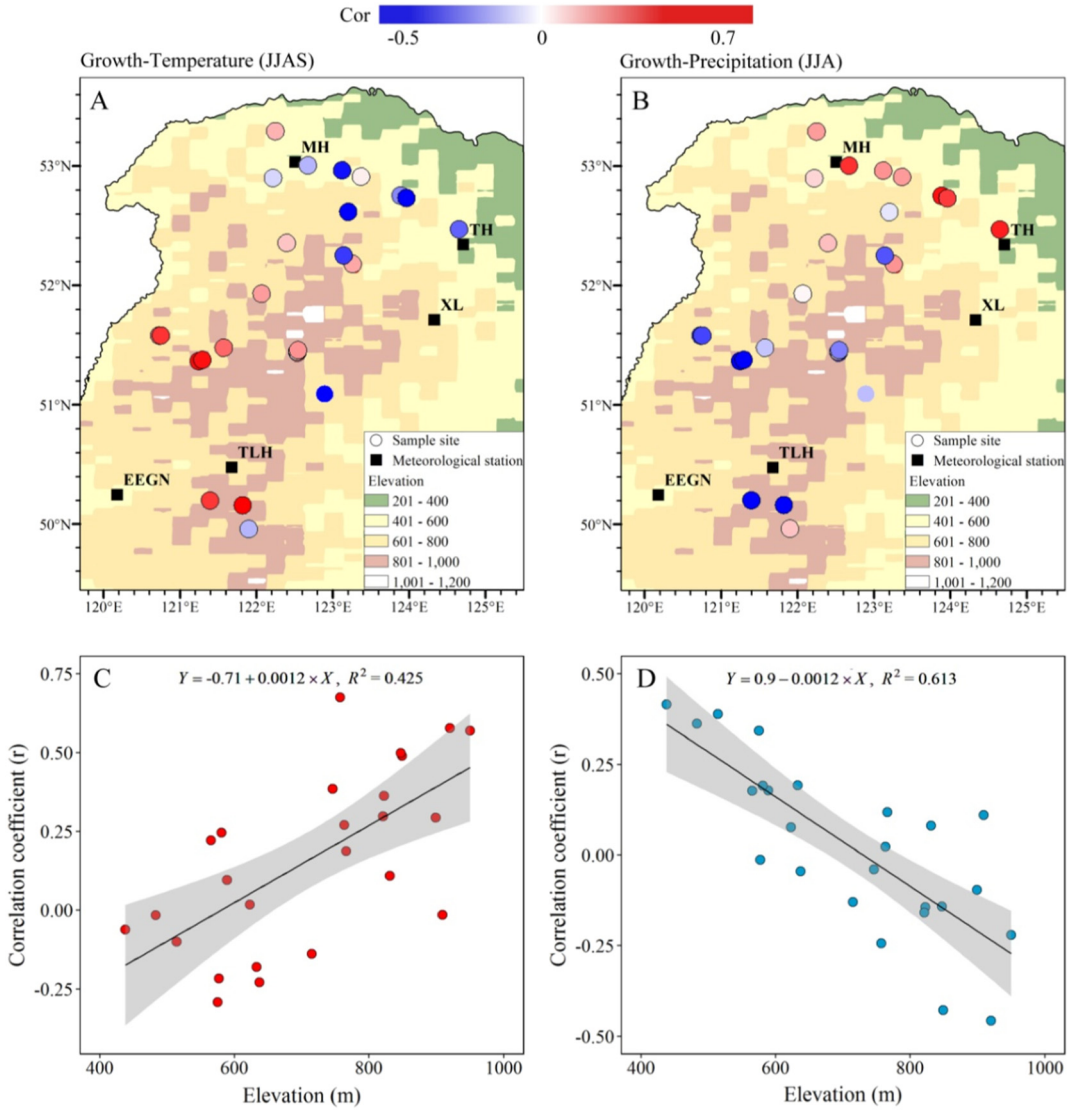

Fig. 7. The correlation-scale between tree growth and climate. Colored dots represent correlations between chronologies and temperature (JJAS, A) and precipitation (JJA, B), ranging from −0.5 (blue) to 0.7 (red). Correlations of growth–temperature (JJAS, C) changed from negative to positive whereas growth–precipitation (JJA, D) changed from positive to negative with increased altitude. Solid lines in C and D represent a linear regression model with 95% confidence interval (shaded grey), and both of the two slopes are significant (temperature, $P < 0.001$; precipitation, $P < 0.001$; significance levels were estimated with two-tailed significance tests).

historic increases in active-layer thicknesses (Anisimov et al., 1997; Bockheim et al., 2013). The deepening of the active layer makes it possible for the trees, especially larches, to have sufficient moisture and nutrients (Guo et al., 2015; Reyes and Lougheed, 2015) in the growing season. However, there is less continuous permafrost at low-altitude in the study area, and this aggravates the warming and drying conditions of the forest under a warming climate. In the case of almost constant precipitation (Fig. 1B; 7.7 mm/10a in increase, $P > 0.1$), warming caused increased drought stress and decreased larch growth at low altitude, while high-altitude trees might get sufficient available water to withstand drought stress and benefit the forest growth.

4.2. Altitudinal divergence of growth–climate associations

Although the altitudinal gradient in this study is smooth and slight, variations in altitude are still obvious among the sampling stands (400–950 m a.s.l., $P < 0.01$), with significant micro-climate differences (especially in temperature) across the study region. The effect of altitude on the relationship between tree growth and climate change in this area was not taken into account in many previous studies (e.g., Jiang et al., 2016; Zhang et al., 2016). In the present study, however, we assessed altitude-related changes in the relationships between tree-growth parameters and climate variables under climate warming.

Correlation between tree growth and climate variables showed that temperature in the winter season (October to February) was positively correlated with larch growth in low- and high-altitude stands, but negatively correlated with growth at medium altitude (600–700 m a.s.l.). Most documented data have shown that warm winters benefit tree growth in boreal forests (Linares and Tíscar, 2011; Sidor et al., 2015; Kolář et al., 2017; Matías et al., 2017), this being in concordance with the main body of our results from low- and high-altitude stands (below 600 m and above 700 m a.s.l.), but it was not found in the stands from medium altitude. In spring, April–May temperature is the driving factor for early onset of cambium activity (Linares and Tíscar, 2011; Prislan et al., 2013; Jyske et al., 2014) and photosynthesis (Goodine et al., 2008), promoting the melting of snow (Vaganov et al., 1999; Huang et al., 2010; Opała et al., 2017) and the recovery of ground temperature, and was the main positive influence on tree growth in our sites (76% of sites). In late autumn and winter (October–January), precipitation generally had a positive effect on tree growth along the

altitudinal gradient (74% of all sites). Snow cover from the winter strongly contributes to the water content in the upper soil layer in spring (Zhang et al., 2008; Qin et al., 2016; Zhang et al., 2018b) and it can insulate the soil from freezing air, thereby exerting a relative "heat preservation" effect that protects root systems (Dinis et al., 2016; Qin et al., 2016; Gradel et al., 2017), which may positively affect tree growth in the upcoming growing season. But more snow accumulation will also delay the start of the growing season (Kirdyanov et al., 2003).

March and May precipitation had a divergent growth–climate response along the altitudinal gradient (Fig. 5): March precipitation positively affected tree growth at high altitude and negatively affected tree growth at low altitude; conversely, May precipitation negatively affected tree growth at high altitude and positively affected tree growth at low altitude. There is a complex hydrothermal process, including permafrost thawing and snow melting with the recovery of ground temperature (monthly mean air temperature, March −12.4 °C, April 0.5 °C, May 9.3 °C), occurring in early spring as the growing season commences. In March, the local climate is cold and the trees are still dormant (Fu et al., 2018), with snow cover delaying the start day of the growing season (Kirdyanov et al., 2003; Qin et al., 2016) at low altitude. In May, snow melt and thawing of continuous permafrost results in there being sufficient soil moisture (Baltzer et al., 2014; Qin et al., 2016; Zhang et al., 2018b) at high altitude, but excessive precipitation can cause waterlogging which could negatively affect tree growth by reducing the energy input to forests and killing the root systems that restrain the respiration (Coutts, 1982; Baltzer et al., 2014). At low altitudes in May, earlier snow melt means an earlier water stress on tree growth; also, the degeneration of permafrost can cause a decrease in soil moisture (Baltzer et al., 2014; Zhang et al., 2018b), leading to a water deficit before the pluvial season, and hence radial growth can be more dependent on May precipitation than on precipitation in other months (van Mantgem et al., 2009; Kolář et al., 2017; Kueppers et al., 2017).

The climate of the growing season is the main factor affecting the growth and distribution or novel species assemblages of forests (Bertrand et al., 2011; Zhang et al., 2016). Our results showed a significant spatial shift in the correlations between tree growth and June–September temperature and between growth and June–August precipitation (Fig. 7A, B) along the altitudinal gradients. Similar results of growth and temperature/precipitation have been found in European forests (Babst et al., 2013; Sidor et al., 2015). In the present study, this could be strongly linked/attributed to the variation in permafrost and air temperature along the altitudinal gradient in the study area. At high altitude, a well-developed permafrost and thick snow cover in winter may cause the soil moisture to be near saturation in summer, and temperature as the main limiting factor is most important to the dynamics of alpine tree lines (Zhang et al., 2011; Chen et al., 2013; Li et al., 2017). Thus, high temperatures are conducive to tree growth in the growing season as the low temperature restriction on tree growth is alleviated (Wang et al., 2016) and nutrients and organic matter are released from deeper permafrost (Guo et al., 2015; Reyes and Lougheed, 2015) at high altitude. On the other hand, more precipitation in summer cannot be conducive to tree growth at high altitude, as it can lead to a net cooling effect (Kueppers et al., 2017), root systems can become over-flooded, which inhibits root respiration (Coutts, 1982), nutrients can be lost in runoff, and there can be a reduction in nutrient absorption and tree photosynthesis. Precipitation in the late growth period and early winter can replenish the content of water in permafrost, which will affect tree growth in the following years, and this deserves investigation in the future.

The discontinuous permafrost has suffered rapid and widespread fragmentation or degeneration in low-altitude stands as the climate has warmed in recent decades (Bockheim et al., 2013; Baltzer et al., 2014). The forests with thawing permafrost have undergone a dramatic change in available water and they are facing unprecedented drought stress at the same time, and so they have to adapt to the greater degree of environmental variation. The current precipitation in degenerated permafrost regions is no longer sufficient to meet the water demands of dense forests, and the ongoing water shortage is leading to a net forest loss (Baltzer et al., 2014; Helbig et al., 2016). Therefore, summer precipitation has had a positive effect on tree growth at low altitude, while a higher temperature is likely to exacerbate moisture stress with a negative effect on tree growth at low altitude (Fig. 6). Several studies have shown altitudinal trends in the growth–climate response, such as more negative effects of temperature as altitude diminishes (Linares and Tíscar, 2011; Sidor et al., 2015) due to higher temperatures causing temperature-induced drought stress and a decrease in net photosynthesis, as precipitation has a powerful influence on growth (Driscoll et al., 2005; Vicente-Serrano et al., 2013). With regard to medium altitude (600–700 m a.s.l.)—a transitional area of continuous permafrost and discontinuous permafrost—climate change has resulted in suitable environmental conditions for the long-term growth patterns of Dahurian larch and few climatic signals can be extracted from the tree rings (Fig. 7A, B). For example, medium-altitude Scots pine has been found to have a higher basal area increment than Scots pine at the high or low altitudinal limits in western Europe (Matías et al., 2017), and temperature in June–July has been found to not be a significant influence on tree growth at intermediate sites (Sidor et al., 2015). But our data indicate that this scenario is likely to be short-term and the region will become a drought-controlled area in the future with climate warming. Generally speaking, in Dahurian larch at least, the response of growth to a warming climate is the opposite at high altitude compared to that at low altitude.

4.3. Larch forests potential retreat/expansion under climate warming

The warming climate has caused the southern boundary of the Dahurian larch distribution to retreat northward in the Great Xing'an Mountains (Bu et al., 2008; Leng et al., 2008a, b). Our results show increasing forest growth at high altitude, decreasing growth at low altitude, and an expected rapid decline in tree growth after a period of stable growth for those sites located at medium altitude. Although the temporal changes of temperature (e.g., climate warming) do not directly explain the "altitudinal trends" of larch growth, it can be understood that temperature varies with altitude change and has different effects along the altitudinal gradient. Therefore, we can evaluate the temperature threshold of the shift in the response of growth to climate factors.

The regressions conducted for the effect of (e.g., mean annual) temperature on growth–temperature ($R^2 = 0.266$, $P < 0.01$, JJAS; Fig. 8A) and growth–precipitation ($R^2 = 0.315$, $P < 0.01$, JJA; Fig. 8B) relationships across the study area have significant downward slopes and upward slopes, respectively. With the increase of (mean annual) temperatures, the correlations between tree growth and temperature change from positive to negative, and from negative to positive for precipitation. This is in agreement with the results of the correlations shift on the altitudinal gradient mentioned above. The shift threshold of the regional mean annual temperature for the growth response to temperature and precipitation is ca. −4.05 °C and ca. −4.79 °C, respectively (Fig. 8A and B). The mean annual temperature threshold seems not to have an absolute, clearly physiological significance for tree growth. However, it can be used as a bio-indicator parameter to evaluate how local micro-climate affects forest ecosystems. This means that the forest stands with specific (e.g., mean annual) temperatures lower than the threshold temperature are the areas where Dahurian larch growth is mainly restricted by temperature; conversely, in stands above the threshold temperature, larch growth is controlled by water. In addition, the region with a mean annual temperature of ca. −4 °C is a transitional zone between continuous permafrost and discontinuous permafrost (Cheng, 1984). Consequently, the impact of changes in environmental factors on these larch forests will ultimately depend on the balance between temperature and precipitation changes across this altitudinal gradient in future.

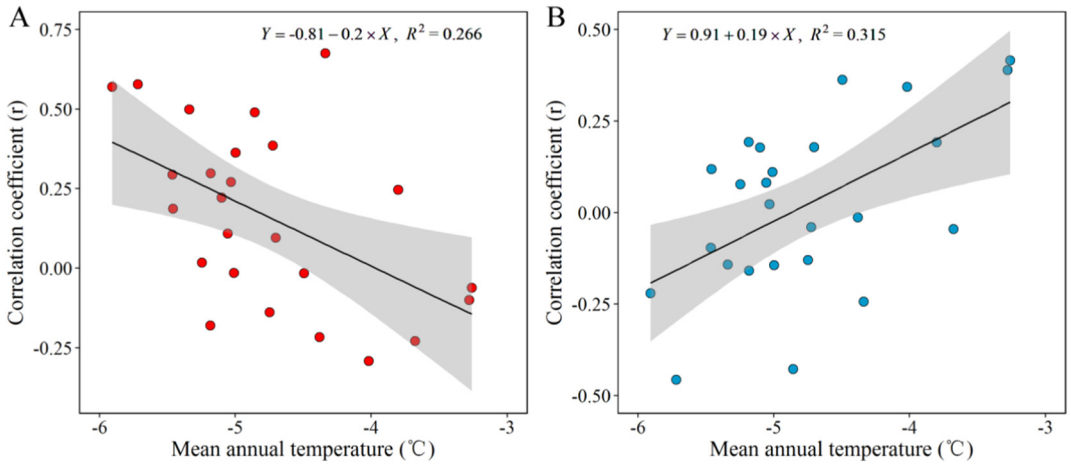

Fig. 8. Changes in the correlation between growth and temperature (Jun–Sep, A)/precipitation (Jun–Aug, B) with increasing mean annual temperature. Solid lines represent a linear regression model with 95% confidence interval (shaded grey).

Based on local larch growth trends and current growth–climate response patterns, we identified contrasting growth–climate responses of larch forests along the altitudinal gradient in the Great Xing'an Mountains: growth increased at high-altitude sites and declined at low-altitude sites, with an anticipated decline after a short-term period of normal growth at medium altitudes under a warmer climate in the future. Although evaluation and anticipation were based on correlation coefficients between radial-growth parameters and climate variables, our results are supported by the hydrothermal gradient and permafrost dynamics of forest stands along the altitudinal gradient in the study area, which would likely lead to upslope expansions for forest distribution similar to many other regions or plant species (Jump et al., 2009; Jiang et al., 2016; Kueppers et al., 2017; Matías et al., 2017). Our methodology also highlights the effects of a mean annual temperature threshold such as −5 to −4 °C for larch growth–climate responses, based on past growth variations, and its use for estimating future forest dynamics and climate sensitivity changes under climate warming.

Supplementary data to this article can be found online at https://doi.org/10.1016/j.scitotenv.2019.03.232.

Credit authorship contribution statement

Xueping Bai: Conceptualization, Formal analysis, Investigation, Writing - original draft, Visualization. **Xianliang Zhang:** Resources, Supervision. **Junxia Li:** Data curation. **Xiaoyu Duan:** Investigation. **Yuting Jin:** Supervision. **Zhenju Chen:** Investigation, Resources, Data curation, Writing - review & editing, Supervision, Project administration, Funding acquisition.

Acknowledgements

We highly appreciate advice by Dr. Lili Wang and Dr. Neil Pederson at the report meeting. We would like to thank Yongxing Chang and Xuepeng Zhao for field work, and also thank Xu Lu for assistance with data analysis.

Funding

This research was funded by the National Natural Science Foundation of China (grant no. 31570632, 41571094, 41601045, 41871027 and 41271066).

References

Anisimov, O.A., Shiklomanov, N.I., Nelson, F.E., 1997. Global warming and active-layer thickness: results from transient general circulation models. Glob. Planet. Chang. 15, 61–77. https://doi.org/10.1016/S0921-8181(97)00009-X.

Babst, F., Poulter, B., Trouet, V., Tan, K., Neuwirth, B., Wilson, R., Carrer, M., Grabner, M., Tegel, W., Levanic, T., Panayotov, M., Urbinati, C., Bouriaud, O., Ciais, P., Frank, D., 2013. Site- and species-specific responses of forest growth to climate across the European continent. Glob. Ecol. Biogeogr. 22, 706–717. https://doi.org/10.1111/geb.12023.

Bai, X., Chang, Y., Zhang, X., Ma, Y., Wu, T., Li, J., Chen, Z., 2016. Impacts of rapid warming on radial growth of *Larix gmelinii* on two typical micro-topographies in the recent 30 years. Chin. J. Appl. Ecol. 27, 3853–3861.

Baltzer, J.L., Veness, T., Chasmer, L.E., Sniderhan, A.E., Quinton, W.L., 2014. Forests on thawing permafrost: fragmentation, edge effects, and net forest loss. Glob. Chang. Biol. 20, 824–834. https://doi.org/10.1111/gcb.12349.

Beckage, B., Osborne, B., Gavin, D.G., Pucko, C., Siccama, T., Perkins, T., 2008. A rapid upward shift of a forest ecotone during 40 years of warming in the Green Mountains of Vermont. Proc. Natl. Acad. Sci. 105, 4197–4202. https://doi.org/10.1073/pnas.0708921105.

Bertrand, R., Lenoir, J., Piedallu, C., Riofrio-Dillon, G., de Ruffray, P., Vidal, C., Pierrat, J.C., Ge'gout, J.C., 2011. Changes in plant community composition lag behind climate warming in lowland forests. Nature 479, 517–520. https://doi.org/10.1038/nature10548.

Bockheim, J., Vieira, G., Ramos, M., López-Martínez, J., Serrano, E., Guglielmin, M., Wilhelm, K., Nieuwendam, A., 2013. Climate warming and permafrost dynamics in the Antarctic Peninsula region. Glob. Planet. Chang. 100, 215–223. https://doi.org/10.1016/j.gloplacha.2012.10.018.

Bu, R., He, H.S., Hu, Y., Chang, Y., Larsen, D.R., 2008. Using the LANDIS model to evaluate forest harvesting and planting strategies under possible warming climates in Northeastern China. For. Ecol. Manage. 254, 407–419. https://doi.org/10.1016/j.foreco.2007.09.080.

Bunn, A.G., 2008. A dendrochronology program library in R (dplR). Dendrochronologia 26, 115–124. https://doi.org/10.1016/j.dendro.2008.01.002.

Chen, I., Hill, J.K., Ohlemüller, R., Roy, D.B., Thomas, C.D., 2011. Rapid range shifts of species associated with high levels of climate warming. Science 333, 1024–1026. https://doi.org/10.1126/science.1206432.

Chen, L., Wu, S., Pan, T., 2011. Variability of climate-growth relationships along an elevation gradient in the Changbai Mountain, northeastern China. Trees - Struct. Funct. 25, 1133–1139. https://doi.org/10.1007/s00468-011-0588-0.

Chen, Z., Zhang, X., He, X., Davi, N.K., Cui, M., Peng, J., 2013. Extension of summer (June–August) temperature records for northern Inner Mongolia (1715–2008), China using tree rings. Quat. Int. 283, 21–29. https://doi.org/10.1016/j.quaint.2012.07.005.

Cheng, G., 1984. Problems on zonation of high-altitude permafrost. Acta Geogr. Sin. 39, 185–193.

Clow, D.W., 2010. Changes in the timing of snowmelt and streamflow in Colorado: a response to recent warming. J. Clim. 23, 2293–2306. https://doi.org/10.1175/2009JCLI2951.1.

Coutts, M.P., 1982. The tolerance of tree roots to waterlogging: V. Growth of woody roots of Sitka Spruce and Lodgepole Pine in waterlogged soil. New Phytol. 90, 467–476. https://doi.org/10.1111/j.1469-8137.1982.tb04479.x.

Dinis, L., Savard, M.M., Gammon, P., Bégin, C., Vaive, J., 2016. Influence of climatic conditions and industrial emissions on spruce tree-ring Pb isotopes analyzed at ppb concentrations in the Athabasca oil sands region. Dendrochronologia 37, 96–106. https://doi.org/10.1016/j.dendro.2015.12.011.

Driscoll, W.W., Wiles, G.C., D'Arrigo, R.D., Wilmking, M., 2005. Divergent tree growth response to recent climatic warming, Lake Clark National Park and Preserve, Alaska. Geophys. Res. Lett. 32, 423–436. https://doi.org/10.1029/2005GL024258.

Fritts, H.C., 1976. Tree Rings and Climate. Academic Press, London.

Fu, Y., He, H., Zhao, J., Larsen, D., Zhang, H., Sunde, M., Duan, S., 2018. Climate and spring phenology effects on autumn phenology in the greater Khingan mountains, northeastern China. Remote Sens. 10, 449–470. https://doi.org/10.3390/rs10030449.

Goodine, G.K., Lavigne, M.B., Krasowski, M.J., 2008. Springtime resumption of photosynthesis in balsam fir (Abies balsamea). Tree Physiol. 28, 1069–1076. https://doi.org/10.1093/treephys/28.7.1069.

Gradel, A., Haensch, C., Ganbaatar, B., Dovdondemberel, B., Nadaldorj, O., Günther, B., 2017. Response of white birch (Betula platyphylla Sukaczev) to temperature and precipitation in the mountain forest steppe and taiga of northern Mongolia. Dendrochronologia 41, 24–33. https://doi.org/10.1016/j.dendro.2016.03.005.
Guo, Y.D., Song, C.C., Wan, Z.M., Lu, Y.Z., Qiao, T.H., Tan, W.W., Wang, L.L., 2015. Dynamics of dissolved organic carbon release from a permafrost wetland catchment in northeast China. J. Hydrol. 531, 919–928. https://doi.org/10.1016/j.jhydrol.2015.10.008.
Harsch, M.A., Hulme, P.E., McGlone, M.S., Duncan, R.P., 2009. Are treelines advancing? A global meta-analysis of treeline response to climate warming. Ecol. Lett. 12, 1040–1049. https://doi.org/10.1111/j.1461-0248.2009.01355.x.
Hartl-Meier, C., Dittmar, C., Zang, C., Rothe, A., 2014. Mountain forest growth response to climate change in the Northern Limestone Alps. Trees - Struct. Funct. 28, 819–829. https://doi.org/10.1007/s00468-014-0994-1.
Helbig, M., Wischnewski, K., Kljun, N., Chasmer, L.E., Quinton, W.L., Detto, M., Sonnentag, O., 2016. Regional atmospheric cooling and wetting effect of permafrost thaw-induced boreal forest loss. Glob. Chang. Biol. 22, 4048–4066. https://doi.org/10.1111/gcb.13348.
Holmes, R.L., 1983. Computer-assisted quality control in tree-ring dating and measurement. Tree-Ring Bull. 43, 69–78. https://doi.org/10.1016/j.ecoleng.2008.01.004.
Huang, J., Tardif, J.C., Bergeron, Y., Denneler, B., Berninger, F., Girardin, M.P., 2010. Radial growth response of four dominant boreal tree species to climate along a latitudinal gradient in the eastern Canadian boreal forest. Glob. Chang. Biol. 16, 711–731. https://doi.org/10.1111/j.1365-2486.2009.01990.x.
IPCC, 2013. Climate Change 2013: The Physical Science Basis. Contribution of Working Group I to the Fifth Assessment Report of the Intergovern-mental Panel on Climate Change [Stocker, T.F., D. Qin, G.-K. Plattner, M. Tignor, S.K. Allen, J. Boschung, A. Nauels, Y. Xia]. Cambridge University Press, Cambridge, United Kingdom and New York, NY, USA.
Jiang, Y., Zhang, J., Han, S., Chen, Z., Setälä, H., Yu, J., Zheng, X., Guo, Y., Gu, Y., 2016. Radial growth response of Larix gmelinii to climate along a latitudinal gradient in the greater Khingan mountains, northeastern China. Forests 7, 295–306. https://doi.org/10.3390/f7120295.
Jump, A.S., Mátyás, C., Peñuelas, J., 2009. The altitude-for-latitude disparity in the range retractions of woody species. Trends Ecol. Evol. 24, 694–701. https://doi.org/10.1016/j.tree.2009.06.007.
Jyske, T., Mäkinen, H., Kalliokoski, T., Nöjd, P., 2014. Intra-annual tracheid production of Norway spruce and Scots pine across a latitudinal gradient in Finland. Agric. For. Meteorol. 194, 241–254. https://doi.org/10.1016/j.agrformet.2014.04.015.
Karl, T.R., Arguez, A., Huang, B., Lawrimore, J.H., McMahon, J.R., Menne, M.J., Peterson, T.C., Vose, R.S., Zhang, H.-M., 2015. Possible artifacts of data biases in the recent global surface warming hiatus. Science 348, 1469–1472.
Kirdyanov, A., Hughes, M., Vaganov, E., Schweingruber, F., Silkin, P., 2003. The importance of early summer temperature and date of snow melt for tree growth in the Siberian Subarctic. Trees - Struct. Funct. 17, 61–69. https://doi.org/10.1007/s00468-002-0209-z.
Kolář, T., Čermák, P., Trnka, M., Žid, T., Rybníček, M., 2017. Temporal changes in the climate sensitivity of Norway spruce and European beech along an elevation gradient in Central Europe. Agric. For. Meteorol. 239, 24–33. https://doi.org/10.1016/j.agrformet.2017.02.028.
Kosaka, Y., Xie, S.P., 2013. Recent global-warming hiatus tied to equatorial Pacific surface cooling. Nature 501, 403–407. https://doi.org/10.1038/nature12534.
Kueppers, L.M., Conlisk, E., Castanha, C., Moyes, A.B., Germino, M.J., de Valpine, P., Torn, M.S., Mitton, J.B., 2017. Warming and provenance limit tree recruitment across and beyond the elevation range of subalpine forest. Glob. Chang. Biol. 23, 2383–2395. https://doi.org/10.1111/gcb.13561.
Leng, W., He, H.S., Bu, R., Dai, L., Hu, Y., Wang, X., 2008a. Predicting the distributions of suitable habitat for three larch species under climate warming in Northeastern China. For. Ecol. Manage. 254, 420–428. https://doi.org/10.1016/j.foreco.2007.08.031.
Leng, W., He, H.S., Liu, H., 2008b. Response of larch species to climate changes. J. Plant Ecol. 1, 203–205. https://doi.org/10.1093/jpe/rtn013.
Li, J., Shi, J., Zhang, D.D., Yang, B., Fang, K., Yue, P.H., 2017. Moisture increase in response to high-altitude warming evidenced by tree-rings on the southeastern Tibetan Plateau. Clim. Dyn. 48, 649–660. https://doi.org/10.1007/s00382-016-3101-z.
Linares, J.C., Tíscar, P.A., 2011. Buffered climate change effects in a Mediterranean pine species: range limit implications from a tree-ring study. Oecologia 167, 847–859. https://doi.org/10.1007/s00442-011-2012-2.
Lyu, L., Suvanto, S., Nöjd, P., Henttonen, H.M., Mäkinen, H., Zhang, Q. Bin, 2017. Tree growth and its climate signal along latitudinal and altitudinal gradients: comparison of tree rings between Finland and the Tibetan Plateau. Biogeosciences 14, 3083–3095. https://doi.org/10.5194/bg-14-3083-2017.
van Mantgem, P.J., Stephenson, N.L., Byrne, J.C., Daniels, L.D., Franklin, J.F., Fulé, P.Z., Harmon, M.E., Larson, A.J., Smith, J.M., Taylor, A.H., Veblen, T.T., 2009. Widespread increase of tree mortality rates in the western United States. Science 323, 521–524. https://doi.org/10.1126/science.1165000.
Martin-Benito, D., Pederson, N., 2015. Convergence in drought stress, but a divergence of climatic drivers across a latitudinal gradient in a temperate broadleaf forest. J. Biogeogr. 42, 925–937. https://doi.org/10.1111/jbi.12462.
Matías, L., Linares, J.C., Sánchez-Miranda, Á., Jump, A.S., 2017. Contrasting growth forecasts across the geographical range of Scots pine due to altitudinal and latitudinal differences in climatic sensitivity. Glob. Chang. Biol. 23, 4106–4116. https://doi.org/10.1111/gcb.13627.
Mátyás, C., 2010. Forecasts needed for retreating forests. Nature 464, 1271. https://doi.org/10.1038/4641271a.
Melvin, T.M., Briffa, K.R., 2008. A "signal-free" approach to dendroclimatic standardisation. Dendrochronologia 26, 71–86. https://doi.org/10.1016/j.dendro.2007.12.001.
Morgan, C., Losey, A., Trout, L., 2014. Late-Holocene paleoclimate and treeline fluctuation in Wyoming's Wind River Range, USA. Holocene 24, 209–219. https://doi.org/10.1177/0959683613516817.
Moritz, C., Agudo, R., 2013. The future of species under climate change: resilience or decline? Science (80-.). 341, 504–508. doi:https://doi.org/10.1126/science.1237190.
Opała, M., Niedźwiedź, T., Rahmonov, O., Owczarek, P., Małarzewski, Ł., 2017. Towards improving the Central Asian dendrochronological network—new data from Tajikistan, Pamir-Alay. Dendrochronologia 41, 10–23. https://doi.org/10.1016/j.dendro.2016.03.006.
Pauli, H., Gottfried, M., Dullinger, S., Abdaladze, O., Akhalkatsi, M., Alonso, J.L.B., Coldea, G., Dick, J., Erschbamer, B., Calzado, R.F., Ghosn, D., Holten, J.I., Kanka, R., Kazakis, G., Kollár, J., Larsson, P., Moiseev, P., Moiseev, D., Molau, U., Mesa, J.M., Nagy, L., Pelino, G., Puşcaş, M., Rossi, G., Stanisci, A., Syverhuset, A.O., Theurillat, J.-P., Tomaselli, M., Unterluggauer, P., Villar, L., Vittoz, P., Grabherr, G., 2012. Recent plant diversity changes on Europe's mountain summits. Science 336, 353–355.
Prislan, P., Gričar, J., de Luis, M., Smith, K.T., Čufar, K., 2013. Phenological variation in xylem and phloem formation in Fagus sylvatica from two contrasting sites. Agric. For. Meteorol. 180, 142–151. https://doi.org/10.1016/j.agrformet.2013.06.001.
Qin, L., Yuan, Y., Zhang, R., Wei, W., Yu, S., Fan, Z., Chen, F., Zhang, T., Shang, H., 2016. Tree-ring response to snow cover and reconstruction of century annual maximum snow depth for northern Tianshan mountains, China. Geochronometria 43, 9–17. https://doi.org/10.1515/geochr-2015-0026.
R Core Team, 2017. R: A language and environment for statistical computing. R Foundation for Statistical Computing, Vienna, Austria. https://www.r-project.org/.
Rabasa, S.G., Granda, E., Benavides, R., Kunstler, G., Espelta, J.M., Ogaya, R., Peñuelas, J., Scherer-Lorenzen, M., Gil, W., Grodzki, W., Ambrozy, S., Bergh, J., Hódar, J.A., Zamora, R., Valladares, F., 2013. Disparity in elevational shifts of European trees in response to recent climate warming. Glob. Chang. Biol. 19, 2490–2499. https://doi.org/10.1111/gcb.12220.
Reyes, F.R., Lougheed, V.L., 2015. Rapid nutrient release from permafrost thaw in arctic aquatic ecosystems. Arct. Antarct. Alp. Res. 47, 35–48. https://doi.org/10.1657/AAAR0013-099.
Salzer, M.W., Hughes, M.K., Bunn, A.G., Kipfmueller, K.F., 2009. Recent unprecedented tree-ring growth in bristlecone pine at the highest elevations and possible causes. Proc. Natl. Acad. Sci. 106, 20348–20353. https://doi.org/10.1073/pnas.0903029106.
Schwörer, C., Henne, P.D., Tinner, W., 2014. A model-data comparison of Holocene timberline changes in the Swiss Alps reveals past and future drivers of mountain forest dynamics. Glob. Chang. Biol. 20, 1512–1526. https://doi.org/10.1111/gcb.12456.
Sidor, C.G., Popa, I., Vlad, R., Cherubini, P., 2015. Different tree-ring responses of Norway spruce to air temperature across an altitudinal gradient in the Eastern Carpathians (Romania). Trees - Struct. Funct. 29, 985–997. https://doi.org/10.1007/s00468-015-1178-3.
Sulman, B.N., Roman, D.T., Yi, K., Wang, L., Phillips, R.P., Novick, K.A., 2016. High atmospheric demand for water can limit forest carbon uptake and transpiration as severely as dry soil. Geophys. Res. Lett. 43, 9686–9695. https://doi.org/10.1002/2016GL069416.
Suvanto, S., Nöjd, P., Henttonen, H.M., Beuker, E., Mäkinen, H., 2016. Geographical patterns in the radial growth response of Norway spruce provenances to climatic variation. Agric. For. Meteorol. 222, 10–20. https://doi.org/10.1016/j.agrformet.2016.03.003.
Tomczak, M., 1998. Spatial interpolation and its uncertainty using automated anisotropic inverse distance weighting (IDW) - cross-validation/jackknife approach. J. Geogr. Inf. Decis. Anal. 2, 18–30.
Vaganov, E.A., Hughes, M.K., Kirdyanov, A.V., Schweingruber, F.H., Silkin, P.P., 1999. Influence of snowfall and melt timing on tree growth in subarctic Eurasia. Nature 400, 149–151. https://doi.org/10.1038/22087.
Vicente-Serrano, S.M., Gouveia, C., Camarero, J.J., Begueria, S., Trigo, R., Lopez-Moreno, J.I., Azorin-Molina, C., Pasho, E., Lorenzo-Lacruz, J., Revuelto, J., Moran-Tejeda, E., Sanchez-Lorenzo, A., 2013. Response of vegetation to drought time-scales across global land biomes. Proc. Natl. Acad. Sci. 110, 52–57. https://doi.org/10.1073/pnas.1207068110.
Wang, Y., Pederson, N., Ellison, A.M., Buckley, H.L., Case, B.S., Liang, E., Camarero, J.J., 2016. Increased stem density and competition may diminish the positive effects of warming at alpine treeline. Ecology 97, 1668–1679. https://doi.org/10.1515/gps-2013-0103.
Wason, J.W., Dovciak, M., 2016. Tree demography suggests multiple directions and drivers for species range shifts in mountains of Northeastern United States. Glob. Chang. Biol. 23, 3335–3347. https://doi.org/10.1111/gcb.13584.
Wei, Z., Jin, H.J., Zhang, J.M., Yu, S.P., Han, X.J., Ji, Y.J., He, R.X., Chang, X.L., 2011. Prediction of permafrost changes in Northeastern China under a changing climate. Sci. China Earth Sci. 54, 924–935. https://doi.org/10.1007/s11430-010-4109-6.
Williams, A.P., Allen, C.D., Macalady, A.K., Griffin, D., Woodhouse, C.A., Meko, D.M., Swetnam, T.W., Rauscher, S.A., Seager, R., Grissino-mayer, H.D., Dean, J.S., Cook, E.R., Gangodagamage, C., Cai, M., Mcdowell, N.G., 2013. Temperature as a potent driver of regional forest drought stress and tree mortality. Nat. Clim. Chang. 3, 292–297. https://doi.org/10.1038/nclimate1693.
Zhang, Y., Ishikawa, M., Ohata, T., Oyunbaatar, D., 2008. Sublimation from thin snow cover at the edge of the Eurasian cryosphere in Mongolia. Hydrol. Process. 22, 3564–3575. https://doi.org/10.1002/hyp.
Zhang, X., He, X., Li, J., Davi, N., Chen, Z., Cui, M., Chen, W., Li, N., 2011. Temperature reconstruction (1750–2008) from Dahurian larch tree-rings in an area subject to permafrost in Inner Mongolia, Northeast China. Clim. Res. 47, 151–159. https://doi.org/10.3354/cr00999.
Zhang, X., Bai, X., Chang, Y., Chen, Z., 2016. Increased sensitivity of Dahurian larch radial growth to summer temperature with the rapid warming in Northeast China. Trees - Struct. Funct. 30, 1799–1806. https://doi.org/10.1007/s00468-016-1413-6.

Zhang, X., Bai, X., Hou, M., Chang, Y., Chen, Z., 2018a. Reconstruction of the regional summer ground surface temperature in the permafrost region of Northeast China from 1587 to 2008. Clim. Chang. 148, 519–531. https://doi.org/10.1007/s10584-018-2212-4.

Zhang, X., Liu, X., Zhang, Q., Zeng, X., Xu, G., Wu, G., Wang, W., 2018b. Species-specific tree growth and intrinsic water-use efficiency of Dahurian larch (*Larix gmelinii*) and Mongolian pine (*Pinus sylvestris* var. *mongolica*) growing in a boreal permafrost region of the Greater Hinggan Mountains, Northeastern China. Agric. For. Meteorol. 248, 145–155. https://doi.org/10.1016/j.agrformet.2017.09.013.